

Original Article

Fatigue and cyclic deformation behavior of non- and boronized austenitic stainless steel AISI 304 at room and elevated temperatures

Tharaphat Wiriyasaroj¹, Patiphan Juijerm^{1*}, Berthold Scholtes², and Thomas Niendorf²

¹ Department of Materials Engineering, Faculty of Engineering,
Kasetsart University, Chatuchak, Bangkok, 10900 Thailand

² Institute of Materials Engineering – Metallic Materials,
University of Kassel, Kassel, D-34125 Germany

Received: 21 August 2017; Revised: 8 November 2017; Accepted: 18 November 2017

Abstract

A thermochemical surface treatment, the powder-packed boronizing process was optimized and then performed on an austenitic stainless steel, AISI 304. Afterwards, boronized specimens were cyclically loaded at ambient and elevated temperatures (350, 550 and 650 °C). Then the results were compared with the behavior in non-boronized condition. Non-statistically evaluated S-N curves and cyclic deformation curves were investigated and are discussed. It was found that the boronizing process only improved the high cycle fatigue (HCF) properties of the austenitic stainless steel AISI 304 at room temperature. An endurance limit of about 340 MPa was observed in the boronized condition, whereas a fatigue strength of about 300 MPa was detected for the non-boronized condition. However, at elevated temperatures boronizing was not associated with enhanced fatigue performance of this steel.

Keywords: fatigue, boronizing, stainless steel, surface treatment

1. Introduction

In many cases, the fatigue performance of technical components is crucial for their safe and reliable applications. Fatigue cracks predominantly initiate at material surfaces due to, e.g., strain localization and local topography effects. Afterwards the cracks propagate into the material (Bannantine *et al.*, 1990; Stephens *et al.*, 1990; Suresh, 1998). Thus, the surface quality and the near surface material state are very important for the fatigue properties of metallic components. If the formation of cracks on the surfaces can be inhibited, enhanced fatigue lifetime should be observed. Many thermochemical surface treatments, e.g., carburizing, nitriding or boronizing, provide a hard layer on the surface. Consequently, improved wear resistance is observed (Davis, 2001; Devaraju

et al., 2012; Gunes & Kanat, 2016; Qin *et al.*, 2017). Moreover, improved fatigue performance - due to increased hardness and compressive residual stresses at the surface after, e.g., a carbonitriding process - is reported by Kanchanomai and Limtrakarn (2008). However, the fatigue lifetime of the boronized plain carbon steel AISI 1010 decreased as compared to the non-boronized condition. This was attributed to the saw-tooth morphology of the boride layer, as reported by Celik *et al.* (2009). On the other hand, for high alloy steels such as tool or stainless steels, smooth morphological boride layers are typically observed (Angkurarach & Juijerm, 2012; Balusamy *et al.*, 2013; Kayali, 2013; Ozdemir *et al.*, 2008; Taktak, 2007). Then, inhibition of surface crack initiation should be expected with such smooth layers of high hardness. Additionally, the boride layer possesses also good oxidation resistance at elevated temperatures (Sinha, 1991). For this reason, the fatigue performance of boronized austenitic stainless steel AISI 304 at room and elevated temperatures is of particular interest. To address this issue, austenitic stainless steel AISI 304 was boronized at 850 °C temperature for

*Corresponding author
Email address: fengppj@ku.ac.th

various durations, and the resulting microstructures of the boride layers were analyzed by optical microscopy as well as by X-ray diffraction (XRD). The boronizing time was investigated and selected to be optimal for the fatigue lifetime at a constant stress amplitude at room temperature. Afterwards, austenitic stainless steel AISI 304 samples were boronized using the optimized boronizing conditions, and then deformed cyclically at both room and elevated temperatures. In addition, cyclic deformation curves were measured and fracture surfaces were analyzed to clarify the fatigue damage process.

2. Materials and Methods

The austenitic stainless steel AISI 304 was delivered as hot-rolled bars with a diameter of 12.5 mm. The chemical composition of this alloy obtained using optical emission spectroscopy is 0.045% C, 1.60% Mn, 0.43% Si, 0.031% P, 0.003% S, 18.26% Cr and 8.65% Ni (all values in wt.%). An average grain size of 45 μm in the austenitic structure was detected. Yield and ultimate tensile strengths of 495 MPa and 693 MPa with an elongation of 56% were measured at room temperature. Specimens were prepared by turning to a fatigue testing shape, with a diameter of 6 mm and a gauge length of 18 mm. The surface at the gauge length was additionally ground up to 600 grit SiC paper in order to clean and obtain a smooth surface before the powder-packed boronizing process. Specimens were boronized using Ekabor-I powder (from BorTec GmbH, Germany) in a steel container with a lid and cement seal and heated in an electric furnace under argon atmosphere. The boronizing was performed at 850 $^{\circ}\text{C}$ temperature for about 5, 15 or 30 min, and then the specimens were cooled in air to room temperature. Insignificant grain growth was observed after the optimal boronizing process, possibly because the boronizing temperature was only about 850 $^{\circ}\text{C}$ with a short soaking period. Rotating bending fatigue tests at a given stress amplitude at room temperature were utilized to determine the optimal boronizing time. Specimens for the rotating bending fatigue tests were prepared following the ASTM E466-96 standard. The microstructure of the boride layers was characterized with an optical microscope and the XRD with $\text{CuK}\alpha$ radiation ($l=0.154$ nm), respectively. The non-statistically evaluated S-N curves were investigated using a stress controlled servo-hydraulic tension-compression testing device with a frequency of 5 Hz without mean stress ($R=-1$). For fatigue tests at elevated temperature, specimens were heated under controlled conditions by an inductive heater. In all cases, to achieve homogeneous temperature within the gage volume, the specimens were held at a given temperature for about 10 min before fatigue tests were started. Strain during fatigue tests was measured using capacitive extensometers.

3. Results and Discussion

3.1 Characterization and optimization of the boronized conditions

After boronizing at 850 $^{\circ}\text{C}$ for approximately 5, 15 or 30 min, the respective boride layer thicknesses were about 4, 5.5 and 8.5 μm , as shown in Figure 1. The boride layer got thicker with boronizing time, in accordance with the diffusion

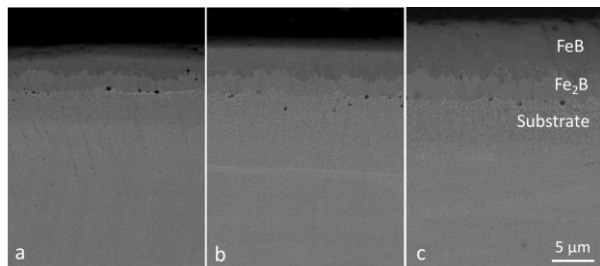


Figure 1. Cross sectional microstructures of the boride layers on the austenitic stainless steel AISI 304 from boronizing for a) 5, b) 15, and c) 30 min.

concept (Juijerm, 2014). Moreover, the formed layers had smooth and compact morphology on the austenitic stainless steel AISI 304 due to the high amount of alloying elements (Qin, 2007; Taktak, 2007). From the XRD patterns shown in Figure 2 and the microstructure visible in Figure 1, it can be concluded that the formed boride layer is of double-phase type, containing FeB and Fe_2B , which is normally detected on metallic materials containing higher amounts of alloying elements such as tool or stainless steels (Angkurarach & Juijerm, 2012; Balusamy *et al.*, 2013; Kayali, 2013; Ozdemir *et al.*, 2008; Taktak, 2007). The outer phase of the boride layer is a FeB layer with a boron content of about 16.23 wt.%, whereas the underlying layer is Fe_2B with a boron content of about 8.83 wt.% (Campos, 2007). The hardness values of the boride layers are relatively high as compared to surfaces treated with a conventional thermochemical process, such as carburizing or nitriding. Hardness values of more than 1800 HV for boride layers on the austenitic stainless steel AISI 304 were measured. The boronized specimens were cyclically deformed at a stress amplitude of 325 MPa at room temperature as shown in Figure 3. The specimens boronized at 850 $^{\circ}\text{C}$ for about 5 or 15 min show higher fatigue lifetime in the high cycle fatigue regime than the non-boronized cases. Therefore, the 5 min boronizing time was selected as optimal and was investigated further for the fatigue lifetime and behavior at room and elevated temperatures.

3.2 Fatigue and cyclic deformation behavior at room temperature

The non-statistically evaluated S-N curves of non- and boronized austenitic stainless steel AISI 304 tested at room temperature are shown in Figure 4. The curves intersect at approximately 2×10^5 loading cycles. For lower numbers of cycles, the non-boronized specimens have higher fatigue strengths than the boronized ones. For higher numbers of loading cycles corresponding to stress amplitudes lower than approximately 350 MPa, the opposite is the case. The non-boronized condition gave fatigue strength of about 300 MPa at 10^6 loading cycles. However, after boronizing the non-statistically evaluated S-N curve shows a higher endurance limit of about 340 MPa, which corresponds to an improvement of the fatigue performance by about 13% from the non-boronized condition. One can assume that crack initiation at the surface in the boronized condition starts early for high applied stress amplitudes in the low cycle fatigue regime. Afterwards, the crack should rapidly spread and

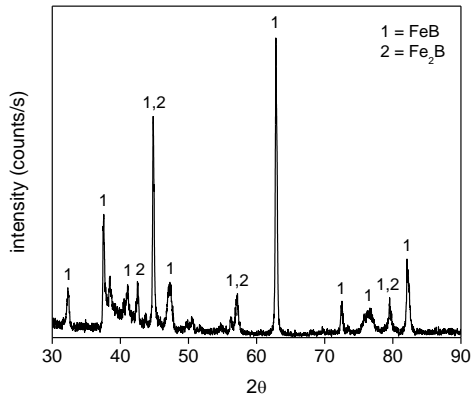


Figure 2. XRD pattern of the austenitic stainless steel AISI 304 boronized at a temperature of 850 °C for about 5 min.

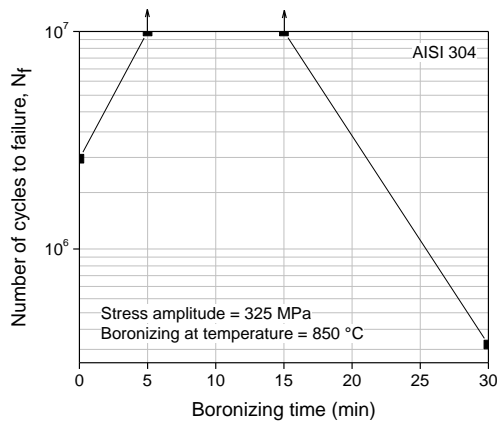


Figure 3. Fatigue lifetime of the boronized stainless steel AISI 304 for different boronizing times.

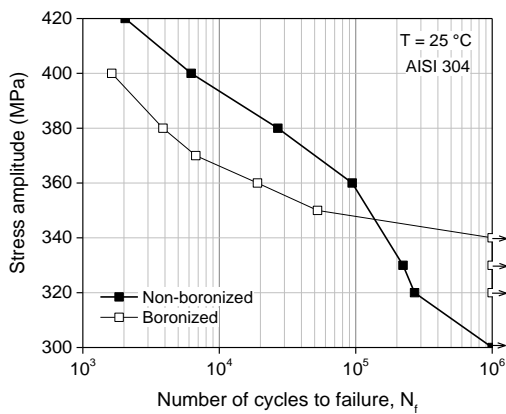


Figure 4. Non-statistically evaluated S-N curves of the non- and boronized austenitic stainless steel AISI 304 at room temperature.

propagate around the specimen due to the high hardness and low ductility of the boride layer, with high stress concentration at the crack tip. Accordingly, this leads to the shorter fatigue lives of the boronized cases in the low cycle fatigue regime. Shiozawa (1997) reports similar behavior, when a

carbon steel coated with TiN and CrN was cyclically deformed with high stress amplitude.

Hysteresis loops of the non- and boronized cases are plotted in Figure 5 for a stress amplitude of 380 MPa. It can be seen that the hysteresis loops shift in the direction of positive strains. Thus, positive mean strains build up and increase with fatigue cycles, especially with high stress amplitudes forming cracks in the boride layer. Additionally, heat generation could be a supplementary cause of the cyclic creep for the austenitic stainless steel AISI 304 during fatigue tests (Nikitin & Besel, 2008). Self-generated heat was detected during the fatigue tests, especially if high plastic strain amplitudes occurred, and the temperatures increased from room temperature to about 100 and 240 °C for the non- and boronized cases, respectively. Cyclic deformation curves of the non- and boronized cases for stress amplitudes of 320 MPa and 380 MPa are shown in Figure 6, as examples. Cyclic softening is usually observed during fatigue loading for both non- and boronized cases, particularly at a high given stress amplitude. This cyclic softening behavior is characteristic for austenitic stainless steel AISI 304 (Nikitin & Besel, 2008; Zauter, 1993). Moreover, lower plastic strain amplitude provides higher fatigue lifetime, in accordance with the Coffin-Manson's law (Coffin, 1966; Manson, 1954).

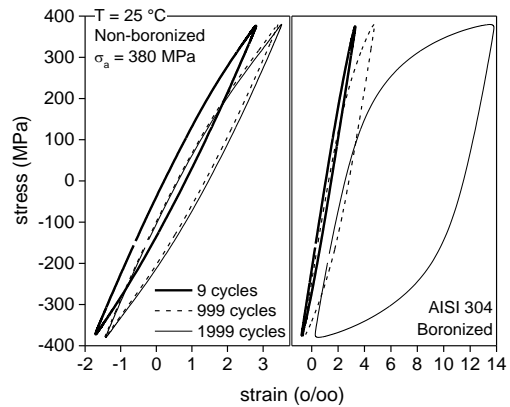


Figure 5. Hysteresis loops of the non- and boronized austenitic stainless steel AISI 304 fatigue at a stress amplitude of 380 MPa at room temperature.

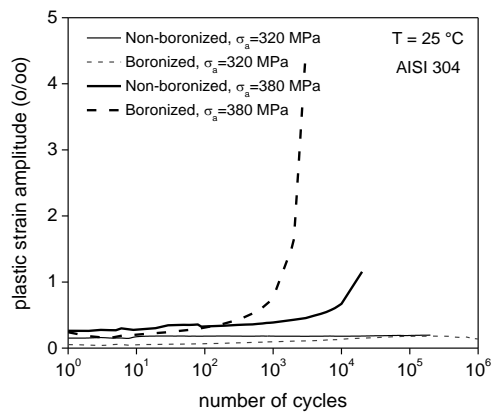


Figure 6. Cyclic deformation curves of the non- and boronized austenitic stainless steel AISI 304 fatigued at applied stress amplitudes of 320 and 380 MPa at room temperature.

3.3 Fatigue and cyclic deformation behavior at elevated temperatures

At the investigated elevated temperatures of 350, 550 and 650 °C, boronized austenitic stainless steel AISI 304 shows shorter fatigue life than in non-boronized condition, even in the high fatigue regime, as illustrated in Figure 7. This becomes more pronounced as the test temperature increases. Only at 350 °C are similar fatigue strengths found for both non- and boronized cases at 10⁶ cycles. It can be assumed that the mechanical properties of the boride layer are deteriorated at elevated temperatures. Yan *et al.* (2001) have shown that the hardness of the iron boride layer decreases considerably at temperatures exceeding 200 °C. Thus, at the tested temperatures 350, 550 and 650 °C, cracks on the surfaces can be initiated early and may propagate quickly, especially in the low cycle fatigue regime (Shiozawa, 1997). This explains the lesser fatigue lives for the boronized cases, observed at elevated temperatures. To assess this hypothesis further, fracture surfaces of the non- and boronized specimens fatigued at a stress amplitude of 280 MPa and at 650 °C were analyzed using a scanning electron microscope (SEM). A characteristic result is shown in Figure 8. It is clearly discernible that crack initiation both for the non- and boronized conditions starts immediately at the surface, but the crack initiation sites are entirely different. In the non-boronized condition, a single crack initiation is observed, whereas multiple crack initiation sites can be seen almost around the boronized specimen. It is possible that firstly, the crack initiated at the boride layer and then rapidly propagated along the hard boride layer in circumferential direction around the boronized specimen. Then multiple crack initiation sites around the boronized specimen are observed, as shown in Figure 8b. Subsequently the crack simultaneously propagated almost around the specimen into the substrate. This mechanism deteriorates the fatigue lifetime of the boronized cases both at room and elevated temperatures. The cyclic deformation behavior at elevated temperatures is comparable to the behavior at room temperature. Cyclic softening is also detected, as shown in Figure 9. The plastic strain amplitudes at elevated temperatures are higher than those measured at room temperature with comparable applied stress amplitudes. This is in agreement with the lower fatigue lives at elevated temperatures implied by Coffin-Manson's law. The hysteresis loops of the non- and boronized cases at elevated temperatures are shown in Figure 10. They display a trend of moving to the positive side for both cases, and the boronized case shows higher plastic strain amplitudes and mean strains than the non-boronized case. Finally, a schematic diagram of the fatigue crack in non- and boronized cases is presented in Figure 11. In the non-boronized case, cracks initiated on the surface and then a critical crack will propagate further causing failure (Figure 11a). If the cracks occur rapidly on the hard surface, e.g., in the boride layer (Figure 11b) during a relatively high cyclic loading at a given temperature, they will propagate around the specimen and then into the substrate (Figure 8). Consequently, the fatigue lifetime will not be enhanced by boronizing (Figure 4 and 7). However, if the crack is not initiated at the boride layer, enhanced fatigue lifetime of the boronized austenitic stainless steel AISI 304 should be detected (Figure 11c).

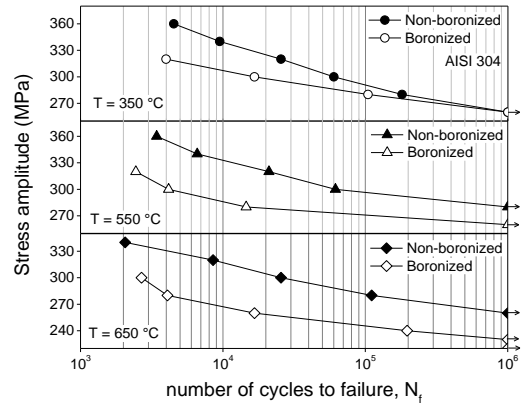


Figure 7 Non-statistically evaluated S-N curves of the non- and boronized austenitic stainless steel AISI 304 at given temperatures of 350, 550 and 650 °C.

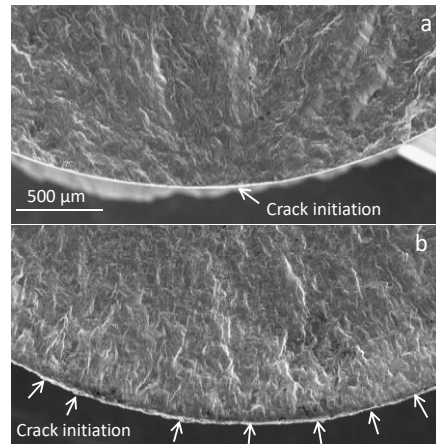


Figure 8. Fracture surfaces of a) non-boronized and b) boronized specimens fatigued at a stress amplitude of 280 MPa at 650 °C.

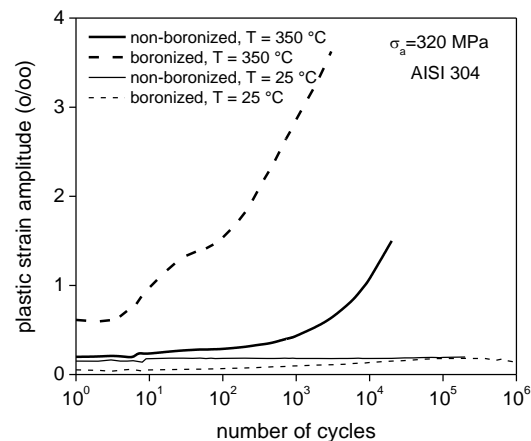


Figure 9. Cyclic deformation curves of non- and boronized austenitic stainless steel AISI 304 fatigued at an applied stress amplitude of 320 MPa at temperatures of 25 and 350 °C.

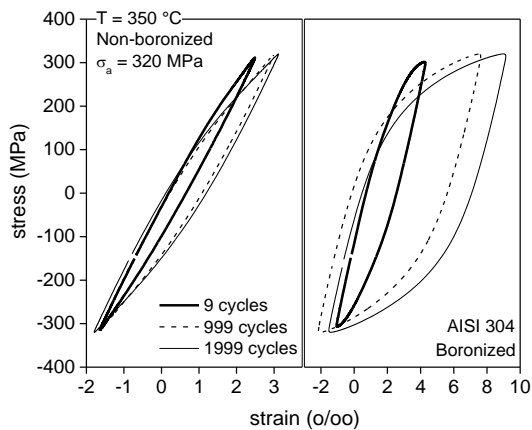


Figure 10. Hysteresis loops of the non- and boronized austenitic stainless steel AISI 304 at a stress amplitude of 320 MPa and 350 °C.

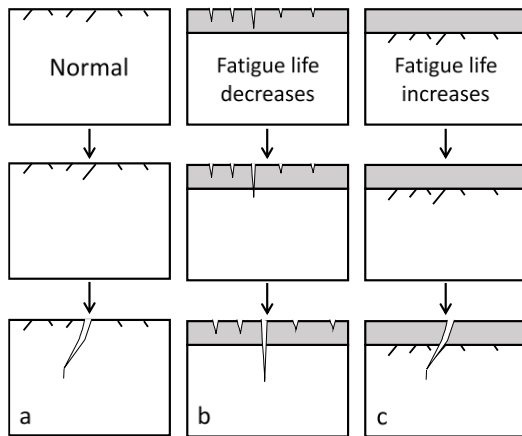


Figure 11. Schematic illustration of crack initiation in a) non-boronized and b) boronized stainless steel AISI 304 with deterioration of fatigue lifetime, and c) the case with enhanced fatigue resistance.

4. Conclusions

In this investigation, the fatigue and cyclic deformation behaviors of non- and boronized austenitic stainless steel AISI 304 at room temperature and at elevated temperatures of 350, 550 and 650 °C were analyzed. The following conclusions can be drawn:

1. A double phase boride layer with FeB and Fe₂B and a thickness of about 4 – 7 μm has been detected on the austenitic stainless steel AISI 304 after boronizing at a temperature of 850 °C for about 5 min.

2. At room temperature, the boride layer on the austenitic stainless steel AISI 304 can enhance the fatigue strength in the high cycle fatigue regime or at low applied stress amplitudes without crack initiation in the boride layer.

3. The boride layer on the austenitic stainless steel AISI 304 will be deteriorated at elevated temperatures, with a consequently poorer fatigue lifetime for the boronized cases than for the non-boronized cases.

4. Cyclic deformation behavior of the non- and boronized austenitic stainless steel AISI 304 show cyclic

softening with increasing positive mean strain under cyclic loading with a frequency of 5 Hz. Increasing stress amplitude and test temperature increase the plastic strain amplitude, while the fatigue lifetime decreases in accordance with the Coffin-Manson's law.

Acknowledgements

The authors would like to thank the Hessen State Ministry of Higher Education, Research and the Arts - Initiative for the Development of Scientific and Economic Excellence (LOEWE) - for financial support of the special research project "Safer Materials". Thanks are also due to Ms. S. Chuemseri for experimental work.

References

- Angkurarach, L., & Juijerm, P. (2012). Effects of direct current field on powder-packed boriding process on martensitic stainless steel AISI 420. *Archives of Metallurgy and Materials*, 57(3), 799-804. doi:10.2478/v10172-012-0087-3
- Balusamy, T., Narayanan, T. S. N. S., Ravichandran, K., Park, I. S., & Lee, M. H. (2013). Pack boronizing of AISI H11 tool steel: Role of surface mechanical attrition treatment. *Vacuum*, 97, 36-43. doi:10.1016/j.vacuum.2013.04.006
- Bannantine, J. A., Comer, J. J., & Handrock J. L. (1990). *Fundamentals of metal fatigue analysis*. New Jersey, Upper Saddle River, NJ: Prentice-Hall.
- Campos, I., Ramirez, G., Figueroa, U., & Velazquez, C. V. (2007). Paste boriding process: evaluation of boron mobility on borided steels. *Surface Engineering*, 23(3), 216-222. doi:10.1179/174329407x174416
- Celik, O. N., Gasan, H., Ulutan, M., & Saygin M. (2009). An investigation on fatigue life of borided AISI 1010 steel. *Journal of Achievements in Materials and Manufacturing Engineering*, 32(1), 13-17.
- Coffin L. F. (1954). A study of the effects of cyclic thermal stresses on a ductile metal. *Transactions of the American Society of Mechanical Engineers*, 76.
- Davis, J. R. (2001). *Surface engineering for corrosion and wear resistance*. Novelty, OH: ASM International.
- Devaraju, A., Elayaperumal, A., Alphonso, J., Kailas, S. V., & Venugopal, S. (2012). Microstructure and dry sliding wear resistance evaluation of plasma nitrided austenitic stainless steel type AISI 316LN against different sliders. *Surface and Coatings Technology*, 207, 406-412. doi:10.1016/j.surfcoat.2012.07.031
- Gunes, I., & Kanat, S. (2016). Investigation of wear behavior of borided AISI D6 steel. *Materiali in Tehnologije*, 50(4), 505-510. doi:10.17222/mit.2014.279
- Juijerm, P. (2014). Diffusion kinetics of different boronizing processes on martensitic stainless steel AISI 420. *Kovove Materialy-Metallic Materials*, 52(4), 231-236. doi:10.4149/km_2014_4_231
- Kanchanomai, C., & Limtrakarn, W. (2008). Effect of residual stress on fatigue failure of carbonitrided low-carbon steel. *Journal of Materials Engineering and Performance*, 17(6), 879-887. doi:10.1007/s11665-008-9212-x

- Kayali, Y. (2013). Investigation of the diffusion kinetics of borided stainless steels. *Physics of Metals and Metallography*, 114(12), 1061-1068. doi:10.1134/S0031918x1322002x
- Manson, S. S. (1966). Thermal stress and low cycle fatigue. New York, NY: McGraw-Hill.
- Nikitin, I., & Besel, M. (2008). Effect of low-frequency on fatigue behaviour of austenitic steel AISI 304 at room temperature and 25 degrees C. *International Journal of Fatigue*, 30(10-11), 2044-2049. doi:10.1016/j.ijfatigue.2008.02.005
- Ozdemir, O., Omar, M. A., Usta, M., Zeytin, S., Bindal, C., & Ucisik, A. H. (2008). An investigation on boriding kinetics of AISI 316 stainless steel. *Vacuum*, 83(1), 175-179. doi:10.1016/j.vacuum.2008.03.026
- Qin, X. J., Guo, X. L., Lu, J. Q., Chen, L. Y., Qin, J. N., & Lu, W. J. (2017). Erosion-wear and intergranular corrosion resistance properties of AISI 304L austenitic stainless steel after low-temperature plasma nitriding. *Journal of Alloys and Compounds*, 698, 1094-1101. doi:10.1016/j.jallcom.2016.12.164
- Shiozawa, K. (1997). Some affecting factors for fatigue strength of ceramics coating steel. *Transactions on Engineering Sciences*, 17. doi:10.2495/SURF970221
- Sinha, A. K. (1991). *Boriding (Boronizing) of steels. ASM handbook: Heat treating: Vol. 4.*, Novelty, OH: ASM International.
- Stephens, R. I., Fatemi, A., Stephens, R. R., & Fuchs, H. O. (2001). *Metal fatigue in engineering*. Ontario, Canada: John Wiley and Sons.
- Suresh, S. (1998). *Fatigue of materials*. Cambridge, England: University Press Cambridge.
- Taktak, S. (2007). Some mechanical properties of borided AISI H13 and 304 steels. *Materials and Design*, 28(6), 1836-1843. doi:10.1016/j.matdes.2006.04.017
- Yan, P. X., Zhang, X. M., Xu, J. W., Wu, Z. G., & Song, Q. M. (2001). High-temperature behavior of the boride layer of 45# carbon steel. *Materials Chemistry and Physics*, 71(1), 107-110. doi:10.1016/S0254-0584(01)00270-X
- Zauter, R., Petry, F., Christ, H. -J., & Mughrabi, H. (1993). Thermomechanical fatigue of the austenitic stainless steel AISI304L. In H. Sehitoglu (Ed.), *Thermo-mechanical fatigue behavior of materials, ASTM publication STP 1186* (pp. 70-90). West Conshohocken, PA: ASTM International.